Nanoscale

Accepted Manuscript

This article can be cited before page numbers have been issued, to do this please use: Y. Jiang, Y. Tang and P. Miao, *Nanoscale*, 2019, DOI: 10.1039/C9NR01307E.

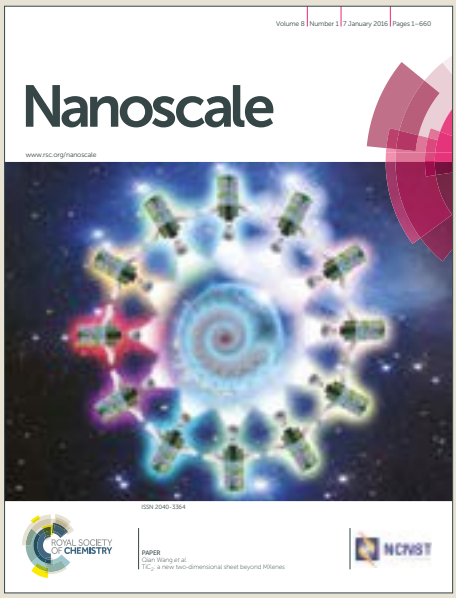

ROYAL SOCIETY OF CHEMISTRY

rsc.li/nanoscale

View Article Online
DOI: 10.1039/C9NR01307E

Nanoscale

COMMUNICATION

Polydopamine nanosphere@silver nanoclusters for fluorescent detection of multiplex tumor markers†

Received 00th January 20xx,
Accepted 00th January 20xx

DOI: 10.1039/x0xx00000x

www.rsc.org/

Yiting Jiang,[abc] Yuguo Tang,[ab] and Peng Miao*[acd]

There is an increasing demand to establish a convenient and stable analytical methodology for screening multiplex tumor markers in early diagnosis of cancers. In this work, an innovative fluorescent method is proposed for simultaneous detection of alpha-fetoprotein (AFP) and carcinoembryonic antigen (CEA). Polydopamine nanosphere@silver nanoclusters (PDAN@AgNCs) system is introduced for fluorescence quenching and recovery. The AgNCs with different emissions are synthesized using different DNA templates, which also contain aptamer sequences towards AFP and CEA, respectively. These single-stranded DNA sequences could be adsorbed on the surface of PDAN through π-π stacking, which result in the quenching of AgNCs. However, in the presence of corresponding tumor marker, aptamer/target complex forms which releases AgNCs from the surface of PDAN and the recovered fluorescence could be used to indicate the concentration of the tumor marker. This PDAN@AgNCs system has been validated preliminarily to screen human serum samples with excellent results. Taking advantages of simplicity, enzyme/antibody-free, low cost and convenient operation, the proposed biosensor has great potential to be used in biomedical researches and clinical diagnosis.

Cancers are currently the world's major public health concern.[1] Precise diagnosis and therapeutic of cancers mainly rely on sensitive measurement of tumor markers, a kind of substances produced and metabolized by tumor cells.[2] Tumor markers always have wide existence and high abundance in tumor tissue, body fluid and serum of cancer patients. For example, carcinoembryonic antigen (CEA) may increase in gastrointestinal tumors, lung cancer, breast cancer, and so on;[3] alpha-fetoprotein (AFP) may increase in liver cancer and malignant teratoma.[4] Researchers have found that the concentrations of CEA and AFP in serum are related to the occurrence of many types of cancers, and the simultaneous detection of the two proteins play an important role in the diagnosis of carcinoma.[5-9] Certain conventional detection methods have already been developed including enzyme-linked immune sorbent assay (ELISA) and chemiluminescence immunoassay (CLIA).[10-11] Despite the good accuracy of these methods, there are still some disadvantages needed to be overcome, such as high cost, time consuming, laborious and complicated operations.

Metal nanoclusters have attracted tremendous attention due to their unique electrical and optical properties, which have been successfully used for various biomedical applications.[12-16] In addition, artificial nucleic acid structures have also been widely designed and manufactured for technological uses.[17-19] Silver nanoclusters (AgNCs), especially water-soluble DNA-templated AgNCs, have fascinating features such as facile synthesis, high quantum yield, tunable fluorescence (FL) emission, narrow photoluminescence band, and great biocompatibility.[20-22] Therefore, AgNCs are ideal candidates for optical materials for biosensing and bioimaging.[23-24] For example, Zhang et al. integrated hairpin DNA-templated AgNCs into strand displacement amplification for miRNA assay.[25] They also employed G-rich fluorescence enhancement effect of AgNCs for miRNA imaging in cancer cells.[26] Zhu et al. developed an enzymatic polymerization-activated AgNC probe for the analysis of apoptosis.[27]

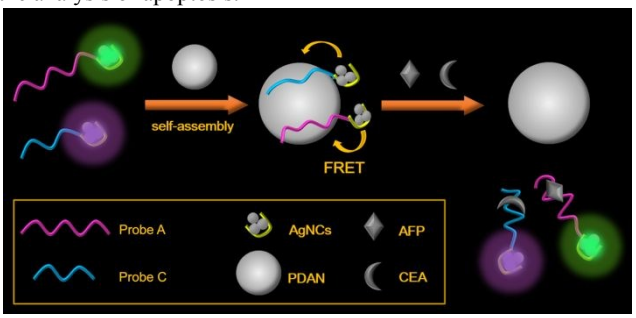

Scheme 1. Illustration of the PDAN@AgNCs based fluorescent biosensor for the detection of multiplex tumor markers.

[a] Suzhou Institute of Biomedical Engineering and Technology, Chinese Academy of Sciences, Suzhou 215163, P. R. China. E-mail: miaopeng@sibet.ac.cn
[b] Jihua Laboratory, Foshan 528200, P. R. China
[c] University of Science and Technology of China, Hefei 230026, P. R. China
[d] Jinan Guokeyigong Science and Technology Development Co., Ltd., Jinan 250103, P. R. China

† Electronic Supplementary Information (ESI) available: Fig. S1-5.

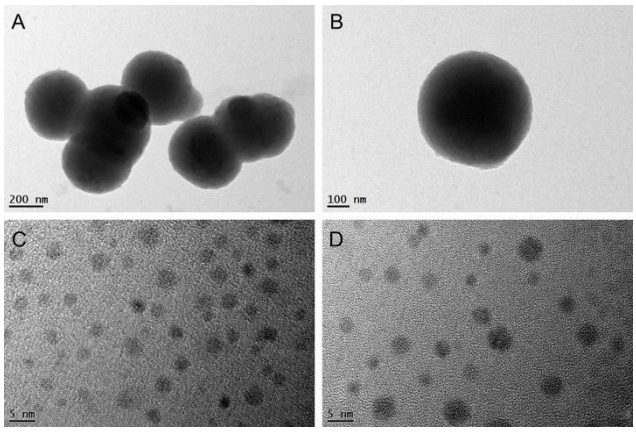

Fig. 1 TEM images of (A) PDANs, (B) a single PDAN, (C) Probe A-templated AgNCs, (D) Probe C-templated AgNCs.

In this work, we have developed a FL platform for the detection of multiplex tumor markers with AgNCs as the signal sources. To achieve selective recognition of target tumor markers, we have replaced traditional antibodies by aptamers, which have smaller sizes but similar binding efficiencies.[28] Aptamers have additional merits like easy synthesis, high stability, reduced immunogenicity, and enhanced tissue penetration.[29] As shown in Scheme 1, we have designed two DNA sequences, Probe A and Probe C, containing aptamers (against AFP and CEA)[30-33] and two different DNA templates for AgNCs with unique optical properties. The synthesized nanoclusters, Probe A-templated AgNCs (A-AgNCs) and Probe C-templated AgNCs (C-AgNCs), are then blended. We have also employed a novel FL quenching material, polydopamine nanosphere (PDAN), which was firstly proposed by Qiang's group in 2014.[34] PDAN shows many promising features like good biocompatibility and broad UV-absorption.[35-36] Most importantly, single-stranded DNA could be adsorbed on the surface of PDAN with strong affinity through π-π stacking.[37] PDAN@AgNCs nanocomposites can thus be facilely formed and FL quenching is achieved through the fluorescence resonance energy transfer (FRET) principle.[38] However, in the presence of target tumor markers, AgNCs could be released from PDAN by forming more stable aptamer/target complex. Therefore, FL could be recovered and the peak intensities can be used to indicate the concentrations of tumor markers. Due to the unique optical properties of A-AgNCs and C-AgNCs, multiplex tumor markers can be detected simultaneously. Therefore, this proposed approach may provide a new tool for early diagnosis of cancers.

The formation of PDAN is through the self-polymerization of dopamine caused by the oxidation of catechins, and the size of the nanosphere increases with longer reaction time.[39] In this study, successful synthesis of PDAN can be confirmed by transmission electron microscopic (TEM) images, in which the size of PDAN is determined to be 274±20.4 nm (Figure 1A and 1B). Two C-rich sequences of Probe A (5'-CCCCCTAATTCCCCC-3') and Probe C (5'-CCCTCCTTCCTCC-3') are used as templates for the synthesis of AgNCs. We have also confirmed the formation of AgNCs by TEM images. As shown in Figure 1C and 1D, both of A-AgNCs and C-AgNCs have excellent water-dispersiblity due to the DNA strands. The AgNCs are spherical with a diameter between 2 and 3 nm. Due to the small sizes, AgNCs may not affect the interaction between aptamer sequences and target proteins.

FL properties of AgNCs are then characterized. As shown in Figure 2A and 2B, the maximum excitation wavelength of A-AgNCs is 500 nm and the maximum emission wavelength is around 570 nm. Different from A-AgNCs, the maximum emission wavelength of C-AgNCs is dependent on the excitation wavelength. With longer excitation wavelength, a red-shift of emission peak is observed and the emission intensity decreases (Figure 2C and 2D). Considering the excitation efficiency for the two AgNCs, we have chosen the excitation/emission of 500 nm/570 nm and 320 nm/364 nm for the following experiments, respectively. The FL of the AgNCs may rely on the DNA template concentrations and reaction times. We have optimized the two parameters by comparing the FL peak intensities and the optimized values include 7 μM Probe A, 5 μM Probe C and 3 h reaction times (Figure S1). The stability of the two AgNCs are also tested. There are no significant decrease in FL intensity after being stored for more than 2 weeks (Figure S2). The quenching effect of PDAN is then studied by employing different amount of PDAN. With the increase of PDAN concentration, the FL peak intensities of both of A-AgNCs and C-AgNCs decrease and reach a plateau with more than 20 μg/mL PDAN (Figure S3). Therefore, 20 μg/mL is selected in the following experiments. To achieve the best analytical performances for the detection of AFP or CEA, the incubation times of tumor markers with PDAN@AgNC system are then studied. With longer time, more aptamers are supposed to be released from the surface of PDAN and the FL peak intensities tend to increase. As expected, both of FL emissions of A-AgNCs and C-AgNCs are enhanced with prolonged reaction time. After 2 h, the FL peaks reach a stable state and the time is chosen for the quantitative analysis (Figure S4).

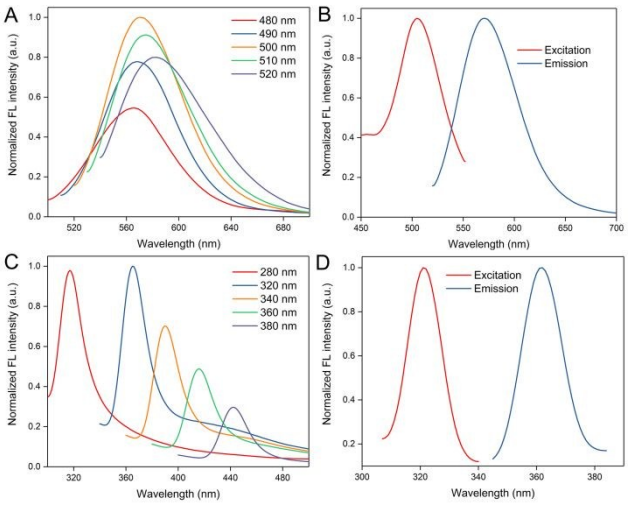

Fig. 2 (A) Fluorescence emission spectra of A-AgNCs excited by a series of wavelengths. (B) Fluorescence emission and excitation spectra of A-AgNCs. (C) (A) Fluorescence emission spectra of C-AgNCs excited by a series of wavelengths. (B) Fluorescence emission and excitation spectra of C-AgNCs.

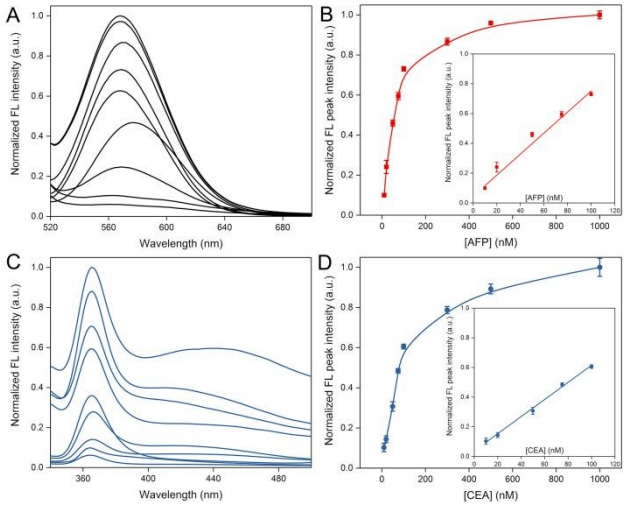

Fig. 3 (A) Fluorescence emission spectra of PDAN@A-AgNCs for the detection of AFP. (B) Calibration curve showing the relationship between FL peak intensity and AFP concentration. Inset shows the linear range. (C) Fluorescence emission spectra of PDAN@C-AgNCs for the detection of CEA. (D) Calibration curve showing the relationship between FL peak intensity and CEA concentration. Inset shows the linear range.

Under optimized experimental conditions, we have evaluated the ability of the proposed method to measure a single tumor marker. The recovery of FL peak intensities are related to the concentration of target tumor markers. As shown in Figure 3, with the increase of the concentrations AFP or CEA from 0 to 1000 nM, the FL spectra gradually increases. Normalized FL intensities at 570 nm and 364 nm are then calculated and two linear relationships are established for the detection of AFP and CEA with a range from 10 to 100 nM, respectively. Two linear fitting equations are as follows.

$$F = 37.217 + 5.831\ c_{AFP}\ (n = 3, R^2 = 0.984)$$

$$F = 32.918 + 5.026\ c_{CEA}\ (n = 3, R^2 = 0.994)$$

The limit of detections for AFP and CEA are 2.4 nM and 5.6 nM, respectively. Since there are no signal amplification processes in the system, the sensitivities are not significantly improved. However, the method is sensitive enough for clinical diagnosis of AFP and CEA. In addition, compared with previous reports, this method shows advantages including simplicity, enzyme/antibody-free, low cost, convenient operation and multiplex targets analysis, which may be beneficial to practical application.[40-41]

We have further blended PDAN@A-AgNCs and PDAN@C-AgNCs to check the performance of multiplex tumor markers analysis. A series of mixed solutions are prepared in which the concentration of AFP and CEA are the same. The samples are then tested by the PDAN@ AgNCs system. As shown in Figure 4A, in the presence of the two tumor markers, FL intensities at the wavelength of 570 nm and 364 nm recover simultaneously. With the increase of the concentration (from 0 to 50 nM), the increasing trends of FL peaks are observed in Figure 4B. In addition, we have also prepared mixed solutions containing AFP and CEA with opposite trends of concentration variations. We have also performed FL measurements to verify the utilization of the PDAN@ AgNCs system. The results in Figure 4C and 4D show excellent conformance to expectation. Therefore, the effectiveness of the fluorescent system for simultaneous analysis of AFP and CEA is confirmed. The distinguishing ability may be originated from the highly specific aptamers against target proteins.

We have then employed human serum samples, which are spiked with the two tumor markers (1 μM). After challenging the biological real samples, the FL responses are compared. Both of A-AgNCs and C-AgNCs show remarkable fluorescence emissions, which are quenched by PDAN with limited emissions. After the introduction of pure AFP and CEA, strong FL recoveries are observed. The tumor markers spiked in serum samples can also result in FL recovery (Figure S5). In addition, we have also applied AgNCs synthesized 2 weeks ago for selective detection of AFP and CEA. The recovered FL intensities are over 93% of original values. These results demonstrate great practical utility of our proposed method.

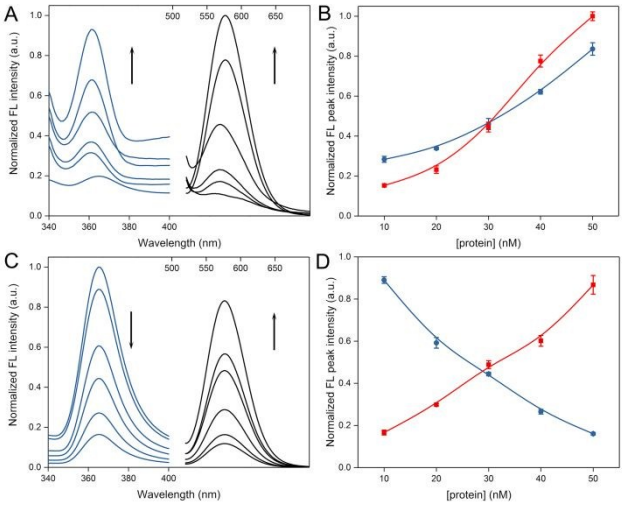

Fig. 4 Fluorescence emission spectra of the PDAN@(A-AgNCs/C-AgNCs) for simultaneous detection of AFP and CEA with (A) the same and (C) different concentrations. (B) and (D) show calibration curves reflecting the relationship between FL intensities (364 nm, 570 nm) and the concentrations of the two tumor markers.

In summary, a novel PDAN/AgNCs-based fluorescent biosensor for simultaneous detection of multiple tumor makers is developed for the first time. PDAN is used as an energy receptor, while two kinds of AgNCs are used as energy donors. Ultrahigh FL quenching ability of PDAN and non-interfering FL recovery of AgNCs make it easy to detect CEA and AFP simultaneously. Moreover, without any sample pretreatment, the proposed strategy shows great potential in actual samples detection. Therefore, our work can be expected to provide a common platform for convenient and multiplex analysis of tumor markers. The application of PDAN@AgNCs may be expanded in early-stage diagnostics and biomedical researches.

Experimental

Materials and instruments

Silver nitrate ($AgNO_3$) was purchased from Shanghai Jiushan Chemicals Co., Ltd. (Shanghai, China). Sodium borohydride ($NaBH_4$) and dopamine hydrochloride were purchased from Sigma (USA). CEA and AFP were purchased from Zhengzhou Biocell Biotechol. Co. Ltd. (Zhengzhou, China). Serum samples were collected from the local hospital (Suzhou, China). Other reagents were of analytical grade and used without further purification. 10 mM Tris–HCl buffer (140 mM NaCl, 5 mM KCl, 1 mM $MgCl_2$ and 1 mM $CaCl_2$, pH 7.4) and 0.2 M phosphate buffer solution (Na_2HPO_4/NaH_2PO_4, pH7.4) were used in this experiment. Double-distilled water was used throughout the experiments, which was purified with a Millipore system with 18 MΩ cm resistivity. DNA probes were synthesized by Sangon Biotechnology Co., Ltd. (Shanghai, China), and their sequences (from 5' to 3') were as following:

Probe A:

TCAGGTGCAGTTCTCGACTCGGTCTTGATGTGGGTAAAAA CCCCCTAATTCCCCC

Probe C:

ATACCAGCTTATTCAATTTATCACGATTAGCCCTCCTTCCT CC

The underlined sequences were aptamers against AFP and CEA, respectively. The oligonucleotides were dissolved in 0.2 M phosphate buffer solution to obtain stock concentrations of 100 μM. Fluorescence spectra were acquired with an F-4600 Fluorescence Spectrophotometer (Hitachi, Japan). Transmission electron microscopic (TEM) images were taken by using a FEI Tecnai G20 transmission electron microscopy (FEI, USA).

Synthesis of PDAN and DNA-templated AgNCs

PDAN was synthesized according to a previous report with minor modifications.[42] Briefly, 100 mg of dopamine hydrochloride was added to a mixture of 100 mL of Tris-buffer (10 mM) and 40 mL of isopropyl alcohol under stirring in the dark. After 48 h, the suspension was centrifuged at 14000 rpm for 10 min and then washed with pure water for several times until the supernatant was clear. The precipitate was then dried for the following experiments.

DNA probes were heated at 95°C for 5 min and then gradually cooled to room temperature over 1 h before use. 6 μL of each DNA probe (100 μM) was mixed with 36 μL of $AgNO_3$ (100 μM) in 0.2 M phosphate buffer solution, followed by whirling for 30 s. After reacting at 4°C for 1 h, $NaBH_4$ (6 μM) was added with vigorous shaking for 1 min. The final volume of the mixture was 600 μL and the molar ratio of DNA : $Ag(NO)_3$: $NaBH_4$ was 1 : 6 : 6. Subsequently, the solution was incubated in dark for 3 h before FL measurements.

Optimization of FL emission and quenching

A-AgNCs and C-AgNCs were excited by a series of excitation wavelengths, and the corresponding emission spectra were recorded and compared. In addition, the FL peak intensities of the synthesized AgNCs were recorded every hour after adding $NaBH_4$ to determine the optimal reaction times. The concentration of DNA templates used for AgNCs synthesis and the concentration of PDAN used for quenching were also optimized by testing a series of concentrations (DNA: 1, 3, 5, 7, 10, 15 μM; PDAN: 0, 3, 6, 10, 16, 20, 30 μg/mL).

Quantitative detection of AFP and CEA

Standard AFP and CEA with a series of concentrations were prepared and mixed with different manners. These tumor markers were then incubated with optimized PDAN@AgNCs system for 2 h. After that, FL emission spectra were measured to test the multiplex analysis performances.

Conflicts of interest

There are no conflicts to declare.

Acknowledgements

This work is supported by the National Natural Science Foundation of China (Grant No. 81771929), the Scientific Research Instrument Developing Project of the Chinese Academy of Sciences (Grant No. YJKYYQ20170067), and the Science and Technology Program of Suzhou (Grant No. SS201867).

Notes and references

1. R. L. Siegel, K. D. Miller and A. Jemal, *CA-Cancer J. Clin.*, 2019, **69**, 7-34.
2. W. X. Li, D. Shu, H. L. Han and Z. F. Ma, *Sens. Actuator B-Chem.*, 2018, **273**, 1451-1455.
3. M. J. Duffy, *Clin. Chem.*, 2006, **52**, 345-351.
4. L. X. Cheng, Z. K. Zhang, D. Zuo, W. F. Zhu, J. Zhang, Q. D. Zeng, D. Y. Yang, M. Li and Y. L. Zhao, *ACS Appl. Mater. Interfaces*, 2018, **10**, 34869-34877.
5. F. Feng, Y. Z. Tian, G. H. Xu, Z. Liu, S. S. Liu, G. Z. Zheng, M. Guo, X. Lian, D. M. Fan and H. W. Zhang, *BMC Cancer*, 2017, **17**, 737.
6. Z. Z. Yu, Y. Tang, G. N. Cai, R. R. Ren and D. P. Tang, *Anal. Chem.*, 2019, **91**, 1222-1226.
7. Z. L. Qiu, J. Shu, J. F. Liu and D. P. Tang, *Anal. Chem.*, 2019, **91**, 1260-1268.
8. W. J. Qin, K. Wang, K. Xiao, Y. F. Hou, W. T. Lu, H. Xu, Y. Wo, S. Q. Feng and D. X. Cui, *Biosens. Bioelectron.*, 2017, **90**, 508-515.
9. J. L. Li, T. Gao, S. Y. Gu, J. Zhi, J. Yang and G. X. Li, *Biosens. Bioelectron.*, 2017, **87**, 352-357.
10. Y. Gao, W. S. Huo, L. Zhang, J. Lian, W. Tao, C. Song, J. P. Tang, S. Shi and Y. H. Gao, *Biosens. Bioelectron.*, 2019, **123**, 204-210.
11. M. Gao, H. Lian, L. J. Yu, M. F. Gong, L. Ma, Y. X. Zhou, M. X. Yu and X. M. Yan, *Anal. Chim. Acta*, 2019, **1048**, 75-84.
12. S. M. Nie and S. R. Emery, *Science*, 1997, **275**, 1102-1106.
13. R. C. Jin, C. J. Zeng, M. Zhou and Y. X. Chen, *Chem. Rev.*, 2016, **116**, 10346-10413.
14. W. X. Hou, F. F. Xia, G. Alfranca, H. Yan, X. Zhi, Y. L. Liu, C. Peng, C. L. Zhang, J. M. de la Fuente and D. X. Cui, *Biomaterials*, 2017, **120**, 103-114.

15. C. L. Zhang, C. Li, Y. L. Liu, J. P. Zhang, C. C. Bao, S. J. Liang, Q. Wang, Y. Yang, H. L. Fu, K. Wang and D. X. Cui, *Adv. Funct. Mater.*, 2015, **25**, 1314-1325.
16. X. L. Zhu, S. Y. Liu, J. P. Cao, X. X. Mao and G. X. Li, *Sci Rep*, 2016, **6**, 19515.
17. D. F. Wang, J. Song, P. F. Wang, V. Pan, Y. W. Zhang, D. X. Cui and Y. G. Ke, *Nat. Protoc.*, 2018, **13**, 2312-2329.
18. T. Schröder, M. B. Scheible, F. Steiner, J. Vogelsang and P. Tinnefeld, *Nano Lett.*, 2019, **19**, 1275-1281.
19. Y. Xu, Y. J. Gao, Y. Y. Su, L. L. Sun, F. F. Xing, C. H. Fan and D. Li, *J. Phys. Chem. Lett.*, 2018, **9**, 6786-6794.
20. W. J. Zhou and S. J. Dong, *Chem. Commun.*, 2017, **53**, 12290-12293.
21. W. J. Zhou, J. B. Zhu, Y. Teng, B. K. Du, X. Han and S. J. Dong, *Nano. Res.*, 2018, **11**, 2012-2023.
22. C. L. Zhang, K. Wang, C. Li, Y. L. Liu, H. L. Fu, F. Pan and D. X. Cui, *J. Mater. Chem. B*, 2014, 6931-6938.
23. C. Y. Li and C. Y. Wei, *Sens. Actuator B-Chem.*, 2017, **240**, 451-458.
24. L. B. Zhang and E. K. Wang, *Nano Today*, 2014, **9**, 132-157.
25. J. P. Zhang, C. Li, G. A. Ramón, Y. L. Liu, C. L. Zhang, F. Pan and D. X. Cui, *Anal. Chem.*, 2016, **88**, 1294-1302.
26. J. P. Zhang, Y. L. Liu, X. Zhi, C. L. Zhang, T. F. Liu and D. X. Cui, *Nanoscale*, 2018, **10**, 11079-11090.
27. R. Zhu, X. Y. Luo, L. Deng, C. Y. Lei, Y. Huang, Z. Nie and S. Z. Yao, *Analyst*, 2018, **143**, 2908-2914.
28. J. H. Zhou and J. Rossi, *Nat. Rev. Drug Discov.*, 2017, **16**, 181-202.
29. R. W. Wang, D. Q. Lu, H. R. Bai, C. Jin, G. B. Yan, M. Ye, L. P. Qiu, R. S. Chang, C. Cui, H. Liang and W. H. Tan, *Chem. Sci.*, 2016, **7**, 2157-2161.
30. C. G. Shao, Y. X. Liu, J. X. Qi, Y. Su, Y. H. Chen, H. G. Xu, Z. K. Lin and H. Q. Guan, *New J. Chem.*, 2018, **42**, 19564-19570.
31. X. X. Zeng, S. S. Ma, J. C. Bao, W. W. Tu and Z. H. Dai, *Anal. Chem.*, 2013, **85**, 11720-11724.
32. Z. H. Zhang, F. H. Duan, J. Y. Tian, J. Y. He, L. Y. Yang, H. Zhao, S. Zhang, C. S. Liu, L. H. He, M. Chen, D. M. Chen and M. Du, *ACS Sens.*, 2017, **2**, 982-989.
33. S. H. Yang, F. F. Zhang, Z. H. Wang and Q. L. Liang, *Biosens. Bioelectron.*, 2018, **112**, 186-192.
34. W. B. Qiang, W. Li, X. Q. Li, X. Chen and D. K. Xu, *Chem. Sci.*, 2014, **5**, 3018-3024.
35. C. P. Wang, D. Wang, T. J. Dai, P. Xu, P. L. Wu, Y. Zou, P. Yang, J. J. Hu, Y. W. Li and Y. Y. Cheng, *Adv. Funct. Mater.*, 2018, **28**, 1802127.
36. Z. Wang, F. Carniato, Y. J. Xie, Y. R. Huang, Y. W. Li, S. He, N. Z. Zang, J. D. Rinehart, M. Botta and N. C. Gianneschi, *Small*, 2017, **13**, 1701830.
37. Y. C. Meng, P. Liu, W. H. Zhou, J. S. Ding and J. W. Liu, *ACS Nano*, 2018, **12**, 9070-9080.
38. W. B. Qiang, H. T. Hu, L. Sun, H. Li and D. K. Xu, *Anal. Chem.*, 2015, **87**, 12190-12196.
39. L. P. Yang, J. H. Kong, D. Zhou, J. M. Ang, S. L. Phua, W. A. Yee, H. Liu, Y. Z. Huang and X. H. Lu, *Chem. Eur. J.*, 2014, **20**, 7776-7783.
40. X. M. Hu, C. Q. Sun, Y. Shi, Y. J. Long and H. Z. Zheng, *New J. Chem.*, 2019, **43**, 4525-4530.
41. Q. L. Wang, H. F. Cui, J. F. Du, Q. Y. Lv and X. J. Song, *RSC Adv.*, 2019, **9**, 6328-6334.
42. W. B. Qiang, X. Wang, W. Li, X. Chen, H. Li and D. K. Xu, *Biosens. Bioelectron.*, 2015, **71**, 143-149.

View Article Online
DOI: 10.1039/C9NR00567E

View Article Online
DOI: 10.1039/C9NR01307E

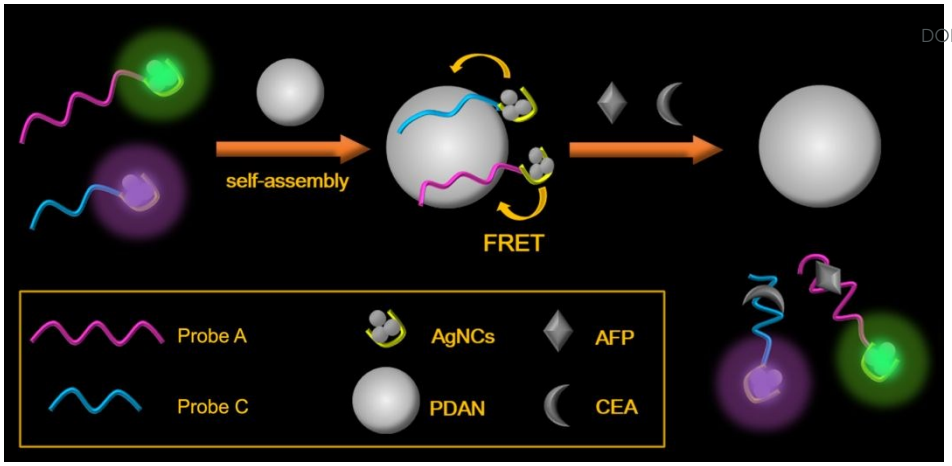

An innovative fluorescent method is developed for simultaneous detection of multiplex tumor markers based on a polydopamine nanosphere@silver nanoclusters system.